

See discussions, stats, and author profiles for this publication at: <https://www.researchgate.net/publication/328057532>

Nutrient acquisition, rather than stress response over diel cycles, drives microbial transcription in a dessicated Namib Desert soil

Preprint · October 2018

DOI: 10.1101/432427

CITATIONS

0

READS

15

4 authors, including:



Carlos León-Sobrino
University of Pretoria

5 PUBLICATIONS 57 CITATIONS

[SEE PROFILE](#)



Jean-Baptiste Ramond

University of Pretoria - Centre for Microbial Ecology and Genomics

125 PUBLICATIONS 427 CITATIONS

[SEE PROFILE](#)



Gillian Maggs-Kölling

Gobabeb Research and Training Centre

7 PUBLICATIONS 2 CITATIONS

[SEE PROFILE](#)

Some of the authors of this publication are also working on these related projects:



Gene expression in a hyper-arid desert; CRISPR-Cas metagenomics [View project](#)



A taxonomic and phylogenetic revision of the genus Ptenopus (Reptilia: Gekkonidae) [View project](#)

1 **Nutrient acquisition, rather than stress response over diel**

2 **cycles, drives microbial transcription in a dessicated Namib**

3 **Desert soil**

4 Carlos León-Sobrino¹, Jean-Baptiste Ramond¹, Gillian Maggs-Kölling² and Don A
5 Cowan^{1*}

6 ¹Centre for Microbial Ecology and Genomics, University of Pretoria, South Africa

7 ²Gobabeb Research and Training Centre, Gobabeb, Namibia

8 *To whom correspondence should be addressed. E-mail don.cowan@up.ac.za

9

10 **Abstract**

11 Hot desert surface soils are characterised by extremely low water activities for large
12 parts of any annual cycle. It is widely assumed that microbial processes in such soils
13 are very limited. Here we present the first metatranscriptomic survey of microbial
14 community function in a low water activity hyperarid desert soil. Sequencing of total
15 mRNA revealed a diverse and active community, dominated by *Actinobacteria*.
16 Metatranscriptomic analysis of samples taken at different times over three days
17 indicated that most functions did not fluctuate on a diel basis, except for a eukaryotic
18 subpopulation which was induced during the cooler night hours. High levels of
19 transcription of chemoautotrophic carbon fixation genes contrasted with limited
20 expression of photosynthetic genes, indicating that chemoautotrophy is an important
21 alternative to photosynthesis for carbon cycling in desiccated desert soils. Analysis of
22 the transcriptional levels of key N-cycling genes provided strong evidence that soil
23 nitrate was the dominant nitrogen input source. Transcriptional network analyses and
24 taxon-resolved functional profiling suggested that nutrient acquisition processes, and
25 not diurnal environmental variation, were the main drivers of community activity in
26 hyperarid Namib Desert soil. While we also observed significant levels of expression of
27 common stress response genes, these genes were not dominant hubs in the co-
28 occurrence network.

29 **Background**

30 Arid lands (deserts) are defined as having a level of precipitation (P) below the
31 potential evapotranspiration (PET) level ($P/PET < 1$). Such lands cover an estimated

32 one-third of Earth's terrestrial surface (Laity, 2008) and are projected to expand in
33 current climate change scenarios (Reich *et al.*, 2001). The Namib Desert, located along
34 the western coast of Namibia and extending into southern Angola and northern South
35 Africa, is the oldest (ca. 5 million years) continuously hyperarid ($P/PET < 0.05$) desert
36 on Earth (Seely and Pallet, 2008).

37 According to current models, aridity results in habitat fragmentation, both
38 geographically leading to "islands" of microbial biomass and diversity and temporally,
39 producing long periods of functional inactivity (Pointing and Belnap, 2012; Collins *et al.*,
40 2014). However, recent evidence suggests that some activity is retained under these
41 extreme conditions (Gunnigle *et al.*, 2017; Schulze-Makuch *et al.*, 2018). In recent
42 years, the microbial ecology of various Namib Desert edaphic niches has been
43 extensively studied (e.g. Scola *et al.*, 2017; Johnson *et al.*, 2017; Ronca *et al.*, 2015;
44 Frossard *et al.*, 2015).

45 RNA sequencing has been employed to study microbial community functional patterns
46 in many different aquatic and terrestrial ecosystems. The short life-span and high
47 turnover of messenger RNA (Belasco and Brawerman, 1993) allows ephemeral states
48 of microbial communities to be captured without significant interference from legacy
49 biomolecules or inactive microbial populations, as might be the case in DNA- or
50 protein-based studies (Nielsen *et al.*, 2006). In desert environments, active community
51 changes over diel cycles or after rainfall have been described by 16S rRNA amplicon
52 transcriptome studies (Gunnigle *et al.*, 2017; Štoviček *et al.*, 2017).

53 In this study, we analyzed 12 shotgun metatranscriptomes from hyperarid desert soils
54 sampled over the course of 3 days. The experiment was designed to assess the diel

55 transcriptional activity of desert edaphic microbial communities, particularly focusing
56 on nutrient acquisition and stress response mechanisms. We also aimed to identify
57 the key community members responsible for nutrient (C, N, P) cycling. Given the
58 fluctuations in light, temperature and humidity to which desert soil communities are
59 exposed within a daily cycle, we hypothesized that functional transcriptional profiles
60 would also show distinct diurnal cycles.

61 **Results and Discussion**

62 **Soil physicochemical characteristics.** Soils were collected from a calcrete gravel plain
63 site near the Gobabeb Research and Training Centre in the central Namib Desert
64 (23°33'34"S 15°02'25"E) (Scholz, 1972) after a prolonged dry period (Supplementary
65 Table S1) . We implemented a three day sampling strategy with soil collection at near
66 sunrise (6:00 h), at midday (12:00 h), at near sunset (18:00 h), and at midnight (24:00
67 h). Surface soil temperatures ranged from 21.4 °C to 51.3 °C, and soil air humidity
68 ranged from 13% to 27.7% (Supplementary Fig. S2). An average photosynthetically
69 active radiation (PAR) of $1722 \pm 22 \mu\text{mol photons m}^{-2} \text{s}^{-1}$ was measured at 12:00 h, but
70 was negligible or zero at 6:00, 18:00, and 24:00 h. Consistent soil respiration was
71 recorded throughout the experiment (Supplementary Table S2).

72 The physicochemistry of soil samples was globally homogeneous. Localized
73 heterogeneity was observed in four quadrats and related mostly to salt or phosphate
74 concentration (Supplementary Table S2, Fig. S3).

75 **Library construction and sequence data.** A sample from each time point was selected
76 for library construction (n=12) based on homogenous soil physicochemical

77 characteristics. Sequencing of cDNA libraries produced 285 million reads in total, with
78 an average read length of 76 nt. After quality filtering and discarding rRNA and human-
79 derived reads, 268 million high-quality reads were retained (Table S3).

80 **Taxonomic composition of the active soil microbial community.** The taxonomic
81 composition of the active microbial populations was similar throughout the study
82 period (Supplementary Fig. S4), in spite of observed variations in temperature,
83 humidity and light (Supplementary Fig. S2, Table S2). A single exception was the Day 2,
84 24:00 h library, which contained an unusually large proportion of fungal (19.5%,
85 compared to an average of 2.8% in the remaining libraries) and *Firmicutes* (38.5%,
86 compared to 5.9%) phylotypic sequences (Supplementary Fig. S4). This result most
87 likely represented a random biological outlier, and this library was excluded from
88 further analyses.

89 The phylogenetic analysis of the remaining 11 libraries showed that members of the
90 domain Bacteria were most active ($94.2 \pm 2.6\%$ of transcripts), with Eukarya
91 comprising $4.3 \pm 1.8\%$ and Archaea $1.5 \pm 1.0\%$. Virus-classified reads amounted to 0.04
92 $\pm 0.02\%$ (Fig. 1A). Despite representing only a minor proportion, this is, to our
93 knowledge, the first report of transcriptionally active viruses in desiccated hot desert
94 soils, where lysogeny is considered to be the dominant state of virus populations
95 (Zablocki *et al.*, 2015). However, the read volume was insufficient to provide a
96 comprehensive survey of transcribed viral genes.

97 Seven bacterial phyla (*Actinobacteria*, *Proteobacteria*, *Firmicutes*, *Bacteroidetes*,
98 *Chloroflexi*, *Cyanobacteria*, and *Deinococcus-Thermus*) and one eukaryal phylum
99 (*Ascomycota*) each contributed more than 1% of the classified reads, jointly comprising

100 93.1 ± 2.3% of the total active community (Fig. 1A and Supplementary Fig. S4). The
101 most active phylum globally was *Actinobacteria*, producing 52.1 ± 5.4% of the classified
102 transcripts, followed by *Proteobacteria*, with 20.2 ± 2.6% of the transcripts. Two
103 prominent actinobacterial families, *Geodermatophilaceae* and *Rubrobacteraceae*,
104 represented 8.2 ± 1.8% and 7.0 ± 1.9%, respectively (Fig. 1A). Both families have been
105 routinely detected in desert soils and their members typically exhibit high stress
106 tolerance and are metabolically versatile (Rainey *et al.*, 2005; Favet *et al.*, 2013;
107 Sghaier *et al.*, 2016; Albuquerque and da Costa, 2014; Normand *et al.*, 2015).

108 **Functional profile of the microbial community.** All core metabolic pathways were
109 transcribed (Fig. 1B), including replication genes, indicating that the active fraction of
110 the soil microbial community had complete functionality.

111 This observation implies the existence of a xeroresistant microbial community in this
112 hyperarid desert niche. Tolerance; i.e., survival with impaired or no activity and no
113 growth, is regarded as the most common strategy adopted by microbial communities
114 under extreme xeric stress, such as in hyperarid desert soils (Lebre *et al.*, 2017).
115 Hyperaridity results in habitat fragmentation and concentrates activity in sheltered
116 "islands of fertility" and during brief wet periods (Pointing and Belnap, 2012; Collins *et al.*,
117 2014). Active microbial populations have recently been detected in hyperarid soils
118 from the Atacama Desert (Schulze-Makuch *et al.*, 2018), although at very reduced
119 activity levels that suggest a temporally or metabolically limited state. However, our
120 transcription results, which demonstrate the presence of a functional fraction of the
121 microbial community, suggest that resistance, rather than tolerance, is a strategy
122 adopted by some of the resident taxa. Resistance is here defined as the maintenance

123 of function, despite the impositions of extreme environmental parameters (i.e.,
124 hyperaridity) (Harrison *et al.*, 2007).

125 The coexistence of desiccation-resistant and -tolerant microbial taxa has been
126 observed in non-arid soils, where Actinobacteria remain active during dry periods
127 whereas Acidobacteria become the dominant active group upon rewetting (Barnard *et*
128 *al.*, 2013). Our findings therefore extend this dual-response model to soils under
129 extreme xeric stress.

130 Genes encoding elements of stress resistance and damage repair mechanisms were
131 highly transcribed. Chaperone genes *groEL* and *dnaK* (4.9% and 1.5% of the classified
132 transcripts, respectively) (Fig. 1B), and protease genes involved in protein quality
133 control (e.g., *clpX/P* and *lon*; 1.7% and 0.7%, respectively) were among the most
134 transcribed. Furthermore, the high relative abundances of peroxisomal orthologs
135 (2.4%), such as superoxide dismutase (SOD) and catalase (*katE*), as well as DNA repair
136 gene transcripts (*recA*, *uvr*, Fig. 1B), support the widely held view that radiation- and
137 desiccation-induced damage (particularly related to oxidation processes) are the major
138 stresses for microbial cells in hyperarid hot desert soils (Makhalanyane *et al.*, 2015).
139 The production of compatible solutes and capsule formation, which are common
140 microbial adaptation mechanisms for desiccation tolerance (Lebre *et al.*, 2017), were
141 suggested by polysaccharide and trehalose biosynthesis gene transcripts such as the
142 alpha-glucan branching enzyme gene *glgB* (0.4% of transcripts) (Rashid *et al.*, 2016)
143 (Fig. 1B). Overall, the transcriptional profile of the microbial community coherently
144 reflects known strategies of desiccation resistance predicted from genomic analyses of

145 desiccation-tolerant microorganisms (Lebre *et al.*, 2017; Schulze-Makuch *et al.*, 2018),
146 allowing full activity of a subpopulation throughout hyperarid periods.

147 **Nutrient cycling and key active taxa.** Carbon, nitrogen, and phosphorus are the major
148 limiting nutrients for microbial communities, and for oligotrophic desert soil
149 communities in particular (Cleveland and Liptzin, 2007; Delgado-Baquerizo *et al.*, 2013;
150 Johnson *et al.*, 2017). The transcriptional activity of orthologs involved in assimilation
151 pathways of these nutrients was thus investigated, to evaluate the contributions of
152 specific taxa to these processes in the community.

153 High levels of functional redundancy were evident (Fig. 2). However, some important
154 ecosystem functions appeared to be taxon-specific. For example, nitrate reductase
155 (*nar*) genes, which encode key enzymes in nitrogen assimilation in soils (Merrick and
156 Edwards, 1995) (Fig. 3A), were transcribed almost exclusively by members of the
157 *Nitrospiraceae* family (Fig. 2A), indicating that this family plays a key role in the
158 nitrogen cycling of Namib desert soil communities.

159 **Nitrogen assimilation.** Nitrogen-fixing bacterial taxa such as *Geodermatophilaceae*,
160 *Frankiaceae* and *Rhizobiales* (Merrick and Edwards, 1995; Sellstedt and Richau, 2013)
161 were among the most active taxa (Fig. 1A). However, transcripts relating to the
162 nitrogen metabolism KEGG pathway represented a small portion (0.2%) of our soil
163 metatranscriptomes and virtually no *nifD* nitrogenase transcripts were detected (Fig.
164 3A). These findings are compatible with recent observations that hypolithic
165 communities, and not surface soil communities, were the primary sources of N₂-
166 fixation in Namib Desert gravel plains (Ramond *et al.*, 2018).

167 Transcriptome data suggested that nitrate reduction, most transcribed by the
168 *Nitrospiraceae* family, and nitrite reduction primarily transcribed in actinobacterial
169 taxa (*nar* and *nir* genes, respectively, Fig. 2A) were the dominant processes in the
170 generation of biologically available nitrogen in the community from a NO_3^- and NO_2^-
171 reservoir (Fig. 3A). These nitrogen species may be accumulated in soils during
172 infrequent wet periods, possibly as a result of the activation of genes and
173 microorganisms inhibited during desiccated conditions (Scherer *et al.*, 1984), or from
174 dry atmospheric deposition processes (Báez *et al.*, 2007; Jia *et al.*, 2016).

175 **Phosphorus and Sulfur assimilation.** Most phosphorus is available to soil microbial
176 communities as inorganic phosphate (Pi), solubilized from the mineral soil fraction or
177 released from organic molecules by the alkaline phosphatase (White and Metcalf,
178 2007). *Pst* phosphate transporter gene transcripts were abundant in the community
179 (1390 average counts per million, cpm). Organic phosphate sources were also possibly
180 exploited, as suggested by transcription of the *phn* phosphonate transporter gene (153
181 cpm) and especially the sn-glycerol 3-phosphate (G3P) transporter gene *ugp* (1228
182 cpm) (Fig. 3B). Although the expression of *phn* and *ugp* can be inhibited by Pi
183 (Schowanek and Verstraete, 1990; Brzoska *et al.*, 1994), organic P utilization may still
184 be an important microbial community trait in oligotrophic desert environments
185 (Vikram *et al.*, 2016). The *ugp* genes were principally transcribed by members of the
186 Order *Rhizobiales* (Class *alpha-Proteobacteria*), potentially replacing Pi transport as a
187 phosphorus acquisition mechanism (Fig. 2B). Plant exudates or membrane
188 phospholipids are possible sources of G3P in soils (Collins *et al.*, 2014; Lidbury *et al.*,
189 2017; Ding *et al.*, 2012). The *glpQ* gene product can cleave these compounds, releasing
190 G3P and triggering activation of the *ugp* transporter genes (Brzoska and Boos, 1988).

191 *GlpQ* is an extracellular enzyme which has been implicated in cooperative interactions
192 between proteobacteria (Lidbury *et al.*, 2017). In our dataset, *glpQ* was mostly
193 transcribed in *Actinobacteria*. The most active actinobacterial family
194 *Geodermatophilaceae*, however, transcribed *glpQ*, but not the G3P transporter *glp* or
195 the alkaline phosphatase *pho* genes, which would dephosphorylate G3P, releasing Pi
196 for its own consumption (Fig. 2B). Our data therefore suggest a putative interaction
197 between *Geodermatophilaceae* and *Rhizobiales*, with the former providing access to
198 phosphorus as G3P for the latter. This interaction may be of considerable importance
199 for desert community maintenance, as both taxa were amongst the most
200 transcriptionally active (8.2% and 6.1%, respectively) (Fig. 1A).

201 Reductive sulfate assimilation (*cys* genes) was the dominant transcribed S-cycling
202 pathway in the community. However, transcripts for the sulfate transporter *cysPUWA*,
203 were mostly associated to proteobacteria, particularly the Burkholderiales family,
204 suggesting a central role of this group in sulfur assimilation and cycling.

205 **Carbon fixation.** A defining feature of arid soils is low productivity and a low organic
206 carbon content (Delgado-Baquerizo *et al.*, 2013). Hyperaridity imposes severe
207 constraints on oxygenic photosynthesis, for which water is the electron donor
208 (Warren-Rhodes *et al.*, 2006). Furthermore, soil communities outside of sheltered
209 fertile islands (i.e., hypoliths, endoliths, or biological soil crusts) typically have a very
210 low abundance of the phototrophic cyanobacteria (Stomeo *et al.*, 2013; Makhalyane
211 *et al.*, 2013). Perhaps not surprisingly, transcription of photosynthetic pathway genes
212 and phototrophic organisms was limited in our dataset (Fig. 1B, Fig. 1A). Notably, reads
213 classified within the Glyoxylate and Dicarboxylate pathway (2.0%) exceeded those

214 assigned to photosynthetic KEGG pathways and, surprisingly, also significantly
215 exceeded those from the TCA Cycle (0.3% and 1.6%, respectively, two-tailed t-test $p <$
216 0.005) (Fig. 1B). We also observed a higher number of transcripts assigned to acetyl-
217 CoA synthetase (ACSS, 9874 cpm) and formate dehydrogenase (FDH, 10254 cpm)
218 compared to RuBisCO (*rbcL/S*, 2672 cpm) (Fig. 1B). These observations strongly suggest
219 that chemoautotrophic ("dark") carbon fixation and/or CO₂ reassimilation mechanisms
220 are important microbial processes by which inorganic C enters the soil microbial
221 community. Chemoautotrophic carbon fixation has been shown as an important
222 process in marine environments, even when photosynthesis is active (Palovaara *et al.*,
223 2014; Aylward *et al.*, 2015), and is a potentially major process in soils (King and Weber,
224 2007; Pratscher *et al.*, 2011). Therefore, we examined the activity of carboxylase genes
225 in greater depth, and their distribution between different families of microorganisms.

226 Although RuBisCO gene transcripts (*rbc*) from the Calvin-Benson-Bassham (CBB) cycle
227 were significant (average 2672 cpm) (Fig. 1B), the majority were assigned to non-
228 photosynthesizing *alpha-Proteobacteria* rather than to *Cyanobacteria* (Fig. 2C). This
229 suggested that the CBB cycle acted predominantly in chemoautotrophic CO₂ fixation or
230 as an electron sink (Badger and Bek, 2008; McKinlay and Harwood, 2010), rather than
231 in photosynthesis.

232 Orthologs of the acetyl-CoA synthase ACSS (9874 cpm), CO dehydrogenase *coxS* (1701
233 cpm) and formate dehydrogenase FDH (10254 cpm) genes, involved in the reductive
234 acetyl-CoA cycle (Wood-Ljungdahl pathway), were significantly transcribed in a wide
235 range of taxa (Fig. 2C). These carboxylases are widely distributed in soil bacteria (King
236 and Weber, 2007) and are active in desert actinobacteria (Sghaier *et al.*, 2016). The

237 activity of these genes in Namib Desert soil microbial communities may be related to
238 the very low energy requirements and the capacity to coassimilate one-carbon
239 compounds or acetate of this pathway (Fuchs, 2011), making it well suited to
240 oligotrophic niches.

241 The reductive citric acid cycle (Arnon-Buchanan cycle) carboxylases *kor* (2-oxoglutarate
242 synthase) and *icd* (isocitrate dehydrogenase) were transcribed by many actinobacterial
243 families, but surprisingly not by *Rubrobacteraceae* (Fig. 2C). Instead, *Rubrobacteraceae*
244 transcribed the acetyl and propionyl-CoA carboxylase *pccB* and *accA/C/D*, the
245 phosphoenolpyruvate (PEP) carboxylase *pckA* and the pyruvate synthase *por*, which
246 participate in other pathways of chemoautotrophic carbon fixation (Fuchs, 2011) (Fig.
247 2C). These pathways could only be partially detected in *Rubrobacteraceae*, as several
248 key genes (e.g., malonyl-CoA reductase, 4-hydroxybutyryl-CoA dehydratase) were not
249 identified. These pathways, either full or partial, allow prokaryotes to coassimilate
250 reduced and uncommon C compounds and to fix carbonate (Fuchs, 2011; Zarzycki and
251 Fuchs, 2011). Our results therefore suggest that the actinobacterial *Rubrobacteraceae*
252 family may be important in inorganic carbon acquisition in desert soils, partly due to a
253 high plasticity in chemoautotrophic metabolism.

254 **Circadian differential gene expression.** Environmental variations often cause microbial
255 communities to exhibit differential activity profiles over temporal timescales (e.g.,
256 daily or seasonally), both in phototrophic and non-phototrophic groups (Klatt *et al.*,
257 2013; van der Meer *et al.*, 2005; Ottesen *et al.*, 2013, 2014; Aylward *et al.*, 2015).

258 Diel transcriptional periodicity was examined using EdgeR (Robinson *et al.*, 2010). Time
259 pairs were contrasted independently, as well as "day" (12:00 and 18:00) versus "night"

260 (24:00 and 6:00) groups as defined by their contrasted temperature and humidity
261 records (Supplementary Fig. S2). Interestingly, pairwise comparisons identified no
262 differentially expressed orthologs ($p > 0.05$) between the 12:00 and 18:00 or between
263 the 24:00 and 6:00 datasets. When "day" and "night" data were contrasted, 13 of 2265
264 orthologs (0.57%) were significantly ($p < 0.05$) induced during the night (Supplementary
265 Table S4). None were highly transcribed orthologs, suggesting that under extreme dry
266 conditions, desert soil communities are generally functionally stable and that their
267 principal functions are not regulated on a diel scale. This conclusion has implications in
268 terms of the perceived drivers of microbial community function, as our results suggest
269 that the constant xeric stress is a more significant driver of *in situ* functionality than
270 daily environmental variations (temperature, air moisture or light). We predict that
271 this functional stability would only be substantially disrupted by stochastic events such
272 as rainfall, which is recognised as a main driver of community assembly and activity in
273 arid soil environments (Belnap *et al.*, 2005; Pointing and Belnap, 2012; Frossard *et al.*,
274 2015; Scola *et al.*, 2017).

275 Surprisingly, we observed a marked enrichment in differentially transcribed eukaryal
276 orthologs, including tubulin, dynein, myosin, SF3B, *dnaJ* and ANP1 genes
277 (Supplementary Table S4). This suggested that the active fungi, which only represented
278 2.8% of the total transcripts, were most active during the cooler and higher
279 atmospheric humidity night hours, contrary to the generally stable activity pattern
280 observed for the rest of the community. This is consistent with observations made on
281 fungi and lichens from arid environments, which appear to grow optimally during small
282 air moisture pulses (Palmer *et al.*, 1987; Jacobson *et al.*, 2015).

283 **Transcriptional network analysis.** The temporal co-variation of KOs was determined in
284 order to examine whether coordinated patterns of gene transcription existed within
285 the soil community. 624 orthologs were used to construct a transcriptional network,
286 83.3% of which (520) clustered into 4 distinct modules (A to D, Fig. 4). The larger
287 clusters A and B were composed of positively interrelated orthologs, although no
288 specific functional enrichment within each module was observed.

289 The principal transcriptional network clusters were connected through three
290 orthologs: the dihydrolipoamide dehydrogenase DLD, the G3P transporter subunit
291 *ugpB* and the glutamate dehydrogenase gene *gudB* genes. These genes occupy
292 network hub positions and therefore changes in their transcriptional status could
293 result in large shifts in community function. The dominant metabolic function
294 associated with the highly transcribed (3917 cpm, Fig. 1B) DLD gene is in the TCA cycle,
295 but has also been shown to affect sugar transport and capsule formation via direct
296 interactions with membrane transporters (Tyx *et al.*, 2011). The importance of
297 exopolysaccharides in desiccation resistance (Lebre *et al.*, 2017), and the TCA cycle in
298 carbon metabolism regulation, support the centrality of DLD in the community
299 network. The gene *ugpB*, as previously discussed, was linked to the rhizobial
300 community as part of a nearly exclusive phosphorus assimilation mechanism (Fig. 2B).
301 The *gudB* gene product catalyzes the synthesis of glutamate, the principal acceptor
302 metabolite in NH₃ assimilation (Merrick and Edwards, 1995)(Fig. 3A).

303 The network was also characterized by a group of orthologs connecting the main
304 clusters A and B. Three of these are involved in nitrogen (*nirA*) (Merrick and Edwards,

305 1995) (Fig. 3A), sulfur (*cysD*) (Pinto *et al.*, 2004) and central carbon metabolism (*scoB*)
306 (Corthésy-Theulaz *et al.*, 1997) (Fig. 1B).

307 Globally, network analysis revealed that transcriptional activity of the community is
308 structured around a selection of hub genes involved in central steps of nitrogen (*nirA*,
309 *gudB*) (Fig. 3A) and sulfate assimilation (*cysD*, *cysN/C*), phosphorus acquisition (*ugpB*)
310 (Fig. 3B) and carbohydrate metabolism (DLD, *scoB*), rather than around genes related
311 to environmental stress resistance and damage repair (e.g. chaperones, proteases,
312 SOD, *uvr*, *rec*), despite these genes being consistently active (Fig. 1).

313 **Conclusions**

314 It is widely accepted that the extreme conditions in hot desert open soils limit both
315 microbial and plant life (Pointing and Belnap, 2012; Makhalanyaane *et al.*, 2015), and
316 that microbial activity is spatially fragmented, temporally limited and water-driven
317 (Pointing and Belnap, 2012; Belnap *et al.*, 2005; Collins *et al.*, 2014). We here show
318 that there is a diverse and consistently active edaphic microbial community in open
319 Namib Desert desiccated soils, dominated by non-photosynthetic bacteria, with a
320 substantial actinobacterial and rhizobial component. Transcripts from all central
321 metabolic pathway genes were detected, suggesting consistent metabolic activity
322 during the study period. We therefore suggest that resistant microbial subpopulations
323 remain active throughout long dry periods, rather than surviving in inactive states.
324 Despite the observation of regular environmental fluctuations, no major diel changes
325 were observed in prokaryotic activity, although a significant activation of fungal genes
326 was noted during the night hours.

327 We identified the key microbial taxa responsible for the variety of strategies for
328 carbon, nitrogen and phosphorus acquisition in the Namib Desert soil. Namely
329 *Nitrospiraceae* (nitrate reduction), *Actinobacteria* (nitrite reduction, carbon fixation)
330 and *alpha-Proteobacteria* (glycerol 3-phosphate assimilation) appeared as key
331 functional members of the soil community.

332 Transcriptional network analysis of the community revealed a group of genes, involved
333 in carbon, nitrogen, phosphorus and sulfur metabolism, in hub positions. This result
334 supports our contention that the main driver of community functionality in Namib
335 gravel plain soil under hyperarid conditions is nutrient assimilation rather than either
336 environmental changes linked to day-night fluctuations (temperature, light, humidity)
337 or the activity of stress resistance and repair genes.

338 Chemoautotrophic carbon fixation genes were among the most transcribed overall,
339 indicating that this constitutes an important form of carbon assimilation under
340 conditions where photosynthesis is restricted. We hypothesize that non-
341 photosynthetic carbon fixation could be a strong adaptive factor in hyperarid, carbon-
342 poor soils. Biochemical evidence is required to quantify the contribution of
343 chemoautotrophy to the microbial community carbon flux.

344 Most notably, microbial N acquisition appeared to be limited to dissimilatory nitrate
345 reduction. While some of the most transcriptionally active actinobacterial and rhizobial
346 taxa are known to possess the capacity for dinitrogen fixation, there was no evidence
347 that this was a significant contribution to nitrogen input budgets under desiccated soil
348 conditions. We suggest that dinitrogen fixation processes may only become significant
349 in times of higher water activity (such as after rainfall).

350 **Materials and Methods**

351 *Sampling procedure*

352 The sampling site was located in the gravel plains of the central Namib Desert
353 (23°33'34"S 15°02'25"E), Namibia, approximately 56 km from the coast. The mean
354 annual precipitation at the site is estimated at 25 mm, principally derived from
355 nocturnal marine fog (Eckardt *et al.*, 2013). A 10 x 10 m experimental plot was sub-
356 divided into 64 quadrats (Supplementary Fig. S1). Surface soils (0-4 cm) were collected
357 at 6 hourly intervals (6:00, 12:00, 18:00, and 24:00 h) over three days from the 12th to
358 the 14th April 2016. Two Hygrochron iButton sensors (Embedded Data Systems,
359 Lawrenceburg KY, USA) were positioned at the corners of the plot, at ~2 cm depth,
360 recording temperature and relative humidity at 4 minute intervals for the length of the
361 experiment (Fig. S1). Soil respiration measurements were performed at the designated
362 sampling times at four points within the plot using a LI-8100 IRGA (LI-COR Biosciences,
363 Lincoln NE, USA), covering an area of 83.7 cm² with a 3 litre chamber for 30 seconds
364 (Supplementary Fig. S1). Photosynthetically active radiation (PAR) was measured using
365 a photometric sensor (Quantum, LI-COR) at the same internal plot locations. Surface
366 soil samples (0-4 cm) were collected at 6 hourly intervals (6:00, 12:00, 18:00, and
367 24:00 h) over three days from the 12th to the 14th April 2016. Three randomly selected
368 quadrats were sampled at each time point (Supplementary Fig. S1). 20 g soil samples
369 were immediately preserved on-site in RNAlater solution (Sigma-Aldrich, St. Louis MO,
370 USA), temporarily stored at -20°C at the Gobabeb Research and Training Center and
371 during transport to the laboratory, and subsequently at -80°C prior to total RNA
372 extraction. An additional 400 g of soil for physicochemical analysis was collected in

373 WhirlPak bags (Nasco, Fort Atkinson WI, USA) and preserved at 4°C before
374 physicochemical analyses. Soil pH, conductivity, cation exchange capacity (CEC), total
375 nitrogen (%N), phosphorus (P), sodium (Na), potassium (K), calcium (Ca), magnesium
376 (Mg), Chloride (Cl), Sulphate (SO₄), ammonium (NH₄) and nitrate (NO₃) contents were
377 analyzed by Bemlab (Pty) Ltd. (<http://www.bemlab.co.za/>; Strand, Western Cape,
378 South Africa) using standard protocols.

379 *Total RNA purification*

380 Soils from twelve physicochemically representative quadrats representing all sampling
381 times were selected for RNA extraction (Supplementary Fig. S1, Table S2). Frozen,
382 RNAlater-preserved soils were thawed at 4°C, centrifuged at 14,500 rpm for 5 minutes
383 and supernatants were discarded. 5 volumes of ice-cold 10 mM Tris-HCl 1 mM EDTA
384 pH 6.5 buffer containing 100 mM NaH₂PO₄ were added to the soil to remove RNAlater
385 salts. The supernatant was discarded after rapid (4 min) centrifugation at 4°C. 0.5
386 volumes lysis buffer (5% CTAB, 0.7 M NaCl, 240 mM KH₂PO₄, pH 8) and an equal
387 volume of TRI Reagent (Sigma-Aldrich) were added, and samples were vortexed at high
388 speed for 30 seconds. RNA purification proceeded according to the manufacturer's
389 instructions. Extracted and purified total RNA was incubated with DNaseI (Invitrogen,
390 Carlsbad, USA) and precipitated in the presence of 20% isopropanol and 15 ng
391 glycogen co-precipitant (GlycoBlue, Invitrogen). RNA concentration and integrity were
392 analysed using a Nanodrop 2000 spectrophotometer (Thermo Scientific, Waltham,
393 USA) and 1% agarose gel electrophoresis. The absence of RT-PCR inhibitors was tested
394 using the Transcriptor cDNA Synthesis Kit v9 (Roche, Indianapolis IN, USA) and
395 universal bacterial 16S rRNA gene primers E9F (5'-GAGTTTGATCCTGGCTCAG-3') and

396 U1510R (5'-GGTTACCTTGTTACGACTT-3') (Reysenbach and Pace, 1995; Hansen *et al.*,
397 1998).

398 *Library construction and sequencing*

399 1 µg DNA-free total RNA from each sample was used for each sequencing library. Due
400 to low RNA yields, we combined RNA from two Day 2 6:00h quadrats (Supplementary
401 Table S1). Construction of rRNA-depleted libraries was carried out with the ScriptSeq
402 Complete Gold Kit (Epidemiology) (Epicentre, Madison WI, USA), following the
403 manufacturer's instructions. Briefly, rRNA was removed by hybridization with bead-
404 immobilized prokaryotic and eukaryotic 28S, 23S, 18S, 16S, 5.8S, 5S, mt16S and mt12S
405 probes prior to RNA fragmentation and reverse transcription with tagged random
406 hexamer primers. cDNA was amplified with TruSeq adaptors containing unique indexes
407 (ScriptSeq Primer Set 1, Epicentre) for 15 PCR cycles. Libraries were purified using
408 AMPure XP beads (Beckman-Coulter, Brea, USA) and final yields were measured with
409 the High Sensitivity dsDNA reagents on a Qubit 2.0 fluorometer (Invitrogen).
410 Multiplexed samples were quality and size analyzed in a High Sensitivity D1000
411 TapeStation (Agilent, Waldbronn, Germany). Libraries were single-end sequenced in a
412 NextSeq500 v2 platform using the NextSeq 500/550 High Output v2 kit (Illumina, San
413 Diego, USA). RNA-seq data were deposited in the ArrayExpress database
414 (www.ebi.ac.uk/arrayexpress) and can be accessed using the reference E-MTAB-6601.

415 Read quality trimming was performed using Prinseq-lite v0.20.4 (Schmieder and
416 Edwards, 2011) on both read ends with a mean Phred value of ≥ 30 in a 6 base sliding
417 window. Reads shorter than 40 bases after trimming were discarded. rRNA and
418 human-derived reads were removed from the dataset using Bowtie2 (Langmead and

419 Salzberg, 2012) with a database of large- and small ribosomal subunit genes from
420 SILVA (<https://www.arb-silva.de/>), 5S rRNA genes from the 5SRNAdb repository
421 (Szymanski *et al.*, 2016) and the GRCh38 human genome primary assembly
422 (ftp://ftp.ncbi.nlm.nih.gov/genomes/archive/old_genbank/Eukaryotes/vertebrates_mammals/Homo_sapiens/GRCh38/seqs_for_alignment_pipelines/GCA_000001405.15_GRCCh38_no_alt_analysis_set.fna.bowtie_index.tar.gz).

425 *Analysis of sequencing reads*

426 Functional and taxonomic profiling, and differential transcription analyses were
427 performed using R version 3.3.3 (R Core Team, 2017). Read taxonomy was inferred
428 from the NCBI Reference Sequence (RefSeq) database, and function was assigned based
429 on the Kyoto Encyclopedia of Genes and Genomes (KEGG) Orthologs (KO) database
430 (Kanehisa *et al.*, 2016) using the MG-RAST server (<http://metagenomics.anl.gov/>)
431 (Meyer *et al.*, 2008). Read count tables were assembled and analysed for temporal
432 expression changes using the EdgeR package (Robinson *et al.*, 2010) for all genes with
433 > 1 count per million (cpm) in at least 3 libraries (n=11). Normalized KEGG ortholog
434 counts were fitted to a generalized log-linear model (*glmQLFit* function) (Robinson and
435 Oshlack, 2010; McCarthy *et al.*, 2012; Lun *et al.*, 2016), and pairwise comparisons
436 between all time points were performed. Additionally, grouped "day" samples from
437 12:00 and 18:00 h were compared to "night" samples from 24:00 and 6:00 h. KOs were
438 considered significantly differentially expressed between time points below a false
439 discovery rate (FDR) corrected p-value threshold of 0.05.

440 Orthologs with average log₂CPM values > 7 were used to construct a transcriptional
441 network (Fig. 5), excluding KEGG categories Human Diseases and Organismal Systems.

442 This threshold was selected as being below the common dispersion value calculated
443 during differential expression analysis in order to reduce interference from high-
444 variance, low-abundance transcripts. A transcriptional network was constructed using
445 MENA's (Deng *et al.*, 2012) RMT-based modeling with a correlation cutoff of 0.900 ($p \leq$
446 0.005). Co-transcription was determined using Pearson's correlation coefficients across
447 libraries (n=11). The network was visualized using Cytoscape v. 3.5.1 (Shannon *et al.*,
448 2003).

449 **Figures**

450 **Fig. 1:** (A) Average transcriptional activity of the 20 most transcriptionally active
451 microbial phyla and families. Phyla are sorted according to their average transcription
452 levels (*aveLogCPM* function). Family transcript abundance is given in average \log_2
453 counts per million ($\log\text{CPM}$). Geod.: *Geodermatophilaceae*; Rub.: *Rubrobacteriaceae*;
454 Methy.: *Methylobacteriaceae*; Rho.: *Rhodobacteraceae*; Brady.: *Bradyrhizobiaceae*;
455 Bac.: *Bacillaceae*; Chroo.: *Chroococcales*; Nostoc.: *Nostocaceae*; Nitrosop.:
456 *Nitrosopumilaceae*; Halobac.: *Halobacteriaceae*. (B) Average transcript abundance of
457 KEGG orthologs in the 40 most transcriptionally active KEGG pathways. Pathways are
458 sorted according to their average \log_2 counts per million (*aveLogCPM* function). Upper
459 KEGG classes are highlighted on the left axis by color: Genetic Information Processing
460 (red), Metabolism (blue) and Environmental Information Processing (green).
461 Categories Human Diseases and Organismal Systems were not included in the plot.
462 Orthologs of particular interest are named, in order of transcript abundance, besides
463 their respective pathway. Abbreviations: ACSL: acyl-CoA synthetase; ACSS: acetyl-CoA
464 synthetase; clpX: Clp protease ATP-binding subunit; *coxS*: carbon-monoxide
465 dehydrogenase small subunit; *cysD*: sulfate adenylyltransferase subunit 2; *cysC*:
466 adenylylsulfate kinase; *cysN/C*: bifunctional enzyme CysN/CysC; DLD: dihydrolipoamide
467 dehydrogenase; *dnaK*: molecular chaperone DnaK; DPO1/3: DNA polymerase I/III;
468 *dppF*: dipeptide transport system ATP-binding protein; FDHa/b: formate
469 dehydrogenase alpha/beta subunit; *fdhA*: formaldehyde dehydrogenase; *glgB*: 1,4-
470 alpha-glucan branching enzyme; *gltB*: glutamate synthase; *groEL*: chaperonin GroEL;
471 *icd*: isocitrate dehydrogenase; *katE*: catalase; *lon*: Lon protease; *pckA*:

472 phosphoenolpyruvate carboxykinase; *rbcl*: ribulose-bisphosphate carboxylase large
473 chain; *recA*: recombination protein RecA; SOD2: superoxide dismutase; *ssb*: single-
474 strand DNA-binding protein; *treS*: maltose alpha-D-glucosyltransferase / alpha-
475 amylase; *uvrA/B*: excinuclease ABC; *xyIA*: xylose isomerase.

476 **Fig. 2:** Correlation between family-level taxonomy and key KEGG ortholog transcription
477 from nitrogen (A), phosphorus (B) and carbon (C) assimilation pathways in selected
478 prokaryotic taxa. (A) Nitrogen metabolism orthologs: *gln*: glutamine synthetase; *glt*:
479 glutamate synthase; *gud*: glutamate dehydrogenase; *nar*: nitrate reductase; *nir*: nitrite
480 reductase. (B) Phosphorus assimilation and G3P metabolism orthologs: *glpD*: glycerol
481 3-phosphate dehydrogenase; *glpK*: glycerol kinase; *glpQ*: glycerophosphodiester
482 phosphodiesterase; *phn*: phosphonate transport; *phoABD*: alkaline phosphatase; *pst*:
483 phosphate transport; *ugp*: sn-glycerol-3-phosphate transport. (C) Carboxylase gene
484 orthologs involved in carbon fixation pathways: *ACSS*: acetyl-CoA synthase; *acc*: acetyl-
485 CoA carboxylase; *FDH*: formate dehydrogenase; *icd*: isocitrate dehydrogenase; *kor*: 2-
486 oxoglutarate synthase; *cox*: CO dehydrogenase; *pcc*: acetyl/propionyl-CoA carboxylase;
487 *pck*: PEP carboxylase; *por*: pyruvate synthase; *rbc*: RuBisCO. Phylum abbreviations: A :
488 *Actinobacteria*; B: *Bacteroidetes*; C: *Cyanobacteria*; Chf: *Chloroflexi*; F: *Firmicutes*;
489 Nitro: *Nitrospirae*; P: *Proteobacteria* (a: alpha, b: beta, d: delta, g: gamma). Only
490 families with > 6 average log₂CPM for the selected genes were included in A and B.
491 Hierarchical clustering of rows and columns was performed with *hclust* function.

492 **Fig. 3:** Community-level transcription of nitrogen (A) and phosphorus (B) assimilation
493 pathways, including glycerol phosphate metabolism. Gene codes in bold highlight the
494 most abundant orthologs from a group performing the same function, when there is a

495 large transcript abundance difference. Numbers below gene codes show the total
496 average counts per million (cpm) of all orthologs. Arrow thickness in each figure is
497 proportional to the indicated cpm value.

498 **Fig. 4:** KEGG ortholog transcriptional network. Only orthologs with average
499 abundances of \log_2 cpm > 7 in the complete dataset were used for computation. Node
500 size is proportional to betweenness centrality and edge thickness is proportional to
501 betweenness. Green or red edge lines indicate a shared positive or negative
502 correlation, respectively. Ortholog abbreviations: ADK: adenosine kinase; *cysD*: sulfate
503 adenyltransferase (sulfate-activating complex); *cysN/C*: bifunctional enzyme
504 *CysN/CysC* (sulfate-activating complex); DLD: dihydrolipoamide dehydrogenase; *gudB*:
505 glutamate dehydrogenase; *ndk*: nucleoside-diphosphate kinase; *nirA*: ferredoxin-nitrite
506 reductase; *pdhC*: pyruvate dehydrogenase; *scoB*: 3-oxoacid CoA-transferase; *ugpB*: sn-
507 glycerol 3-phosphate transport system.

508 **Declarations**

509 *Funding*

510 The authors acknowledge funding support from the University of Pretoria and the
511 South African National Research Foundation (grant number 95565)

512 *Data availability*

513 The dataset supporting the conclusions of this article is available in the ArrayExpress
514 repository, <https://www.ebi.ac.uk/arrayexpress/> (accession no. E-MTAB-6601).

515 *Competing interests*

516 The authors declare no competing financial interests and no conflict of interest.

517 *Author contributions*

518 C. L.-S., J.-B. R. and D. A. C. conceived the experiment. G. M.-K. provided logistical
519 support and field advice in the Namib Desert. C. L.-S. performed all experimental work
520 and bioinformatic analysis of the sequencing output. C. L.-S., J.-B. R. and D. A. C.
521 participated in the interpretation of results and writing of the manuscript. D. A. C.
522 provided funding.

523 *Acknowledgements*

524 The authors wish to thank the Gobabeb Research and Training Station personnel for
525 their assistance, advice and for providing access to their facilities during the sampling
526 process.

527 **References**

528 Albuquerque L, da Costa MS. (2014). The Family Rubrobacteraceae. In: *The*
529 *Prokaryotes*. Springer Berlin Heidelberg: Berlin, Heidelberg, pp 861–866.

- 530 Aylward FO, Eppley JM, Smith JM, Chavez FP, Scholin CA, DeLong EF. (2015). Microbial
531 community transcriptional networks are conserved in three domains at ocean basin
532 scales. *Proc Natl Acad Sci U S A* **112**: 5443–8.
- 533 Badger MR, Bek EJ. (2008). Multiple Rubisco forms in proteobacteria: their functional
534 significance in relation to CO₂ acquisition by the CBB cycle. *J Exp Bot* **59**: 1525–1541.
- 535 Báez S, Fargione J, Moore DJ, Collins SL, Gosz JR. (2007). Atmospheric nitrogen
536 deposition in the northern Chihuahuan desert: Temporal trends and potential
537 consequences. *J Arid Environ* **68**: 640–651.
- 538 Barnard RL, Osborne CA, Firestone MK. (2013). Responses of soil bacterial and fungal
539 communities to extreme desiccation and rewetting. *ISME J* **7**: 2229–2241.
- 540 Belasco JG, Brawerman G. (1993). Control of messenger RNA stability. Academic Press.
- 541 Belnap J, Welter JR, Grimm NB, Barger N, Ludwig JA. (2005). Linkages between
542 microbial and hydrologic processes in arid and semiarid watersheds. *Ecology* **86**: 298–
543 307.
- 544 Brzoska P, Boos W. (1988). Characteristics of a *ugp*-encoded and *phoB*-dependent
545 glycerophosphoryl diester phosphodiesterase which is physically dependent on the
546 *ugp* transport system of *Escherichia coli*. *J Bacteriol* **170**: 4125–35.
- 547 Brzoska P, Rimmele M, Brzostek K, Boos W. (1994). The *pho* regulon-dependent *Ugp*
548 uptake system for glycerol-3-phosphate in *Escherichia coli* is trans inhibited by Pi. *J*
549 *Bacteriol* **176**: 15–20.
- 550 Cleveland CC, Liptzin D. (2007). C:N:P stoichiometry in soil: is there a ‘Redfield ratio’ for
551 the microbial biomass? *Biogeochemistry* **85**: 235–252.

- 552 Collins SL, Belnap J, Grimm NB, Rudgers JA, Dahm CN, D’Odorico P, *et al.* (2014). A
553 Multiscale, Hierarchical Model of Pulse Dynamics in Arid-Land Ecosystems. *Annu Rev*
554 *Ecol Evol Syst* **45**: 397–419.
- 555 Corthésy-Theulaz IE, Bergonzelli GE, Henry H, Bachmann D, Schorderet DF, Blum AL, *et*
556 *al.* (1997). Cloning and characterization of *Helicobacter pylori* succinyl
557 CoA:acetoacetate CoA-transferase, a novel prokaryotic member of the CoA-transferase
558 family. *J Biol Chem* **272**: 25659–67.
- 559 Delgado-Baquerizo M, Maestre FT, Gallardo A, Bowker MA, Wallenstein MD, Quero JL,
560 *et al.* (2013). Decoupling of soil nutrient cycles as a function of aridity in global
561 drylands. *Nature* **502**: 672–676.
- 562 Deng Y, Jiang Y-H, Yang Y, He Z, Luo F, Zhou J. (2012). Molecular ecological network
563 analyses. *BMC Bioinformatics* **13**: 113.
- 564 Ding H, Yip CB, Geddes BA, Oresnik IJ, Hynes MF. (2012). Glycerol utilization by
565 *Rhizobium leguminosarum* requires an ABC transporter and affects competition for
566 nodulation. *Microbiology* **158**: 1369–1378.
- 567 Eckardt FD, Soderberg K, Coop LJ, Muller AA, Vickery KJ, Grandin RD, *et al.* (2013). The
568 nature of moisture at Gobabeb, in the central Namib Desert. *J Arid Environ* **93**: 7–19.
- 569 Favet J, Lapanje A, Giongo A, Kennedy S, Aung Y-Y, Cattaneo A, *et al.* (2013). Microbial
570 hitchhikers on intercontinental dust: catching a lift in Chad. *ISME J* **7**: 850–67.
- 571 Frossard A, Ramond J-B, Seely M, Cowan DA. (2015). Water regime history drives
572 responses of soil Namib Desert microbial communities to wetting events. *Sci Rep* **5**:
573 12263.

- 574 Fuchs G. (2011). Alternative pathways of carbon dioxide fixation: Insights into the early
575 evolution of life? *Annu Rev Microbiol* **65**: 631–658.
- 576 Gunnigle E, Frossard A, Ramond J-B, Guerrero L, Seely M, Cowan DA. (2017). Diel-scale
577 temporal dynamics recorded for bacterial groups in Namib Desert soil. *Sci Rep* **7**: 40189.
- 578 Hansen MC, Tolker-Nielsen T, Givskov M, Molin S. (1998). Biased 16S rDNA PCR
579 amplification caused by interference from DNA flanking the template region. *FEMS*
580 *Microbiol Ecol* **26**: 141–149.
- 581 Harrison JJ, Ceri H, Turner RJ. (2007). Multimetal resistance and tolerance in microbial
582 biofilms. *Nat Rev Microbiol* **5**: 928–938.
- 583 Jacobson K, Van Diepeningen A, Evans S, Fritts R, Gemmel P, Marsho C, *et al.* (2015).
584 Non-rainfall moisture activates fungal decomposition of surface litter in the Namib
585 Sand Sea. *PLoS One* **10**: e0126977.
- 586 Jia Y, Yu G, Gao Y, He N, Wang Q, Jiao C, *et al.* (2016). Global inorganic nitrogen dry
587 deposition inferred from ground- and space-based measurements. *Sci Rep* **6**: 19810.
- 588 Johnson RM, Ramond J-B, Gunnigle E, Seely M, Cowan DA. (2017). Namib Desert
589 edaphic bacterial, fungal and archaeal communities assemble through deterministic
590 processes but are influenced by different abiotic parameters. *Extremophiles* **21**: 381–
591 392.
- 592 Kanehisa M, Sato Y, Kawashima M, Furumichi M, Tanabe M. (2016). KEGG as a
593 reference resource for gene and protein annotation. *Nucleic Acids Res* **44**: D457-62.
- 594 King GM, Weber CF. (2007). Distribution, diversity and ecology of aerobic CO-oxidizing
595 bacteria. *Nat Rev Microbiol* **5**: 107–118.

- 596 Klatt CG, Liu Z, Ludwig M, Kühl M, Jensen SI, Bryant DA, *et al.* (2013). Temporal
597 metatranscriptomic patterning in phototrophic Chloroflexi inhabiting a microbial mat
598 in a geothermal spring. *ISME J* **7**: 1775–1789.
- 599 Laity J. (2008). *Deserts and desert environments*. Wiley-Blackwell: Chichester, UK.
- 600 Langmead B, Salzberg SL. (2012). Fast gapped-read alignment with Bowtie 2. *Nat*
601 *Methods* **9**: 357–359.
- 602 Lebre PH, De Maayer P, Cowan DA. (2017). Xerotolerant bacteria: surviving through a
603 dry spell. *Nat Rev Microbiol* **15**: 285–296.
- 604 Lidbury IDEA, Murphy ARJ, Fraser TD, Bending GD, Jones AME, Moore JD, *et al.* (2017).
605 Identification of extracellular glycerophosphodiesterases in *Pseudomonas* and their
606 role in soil organic phosphorus remineralisation. *Sci Rep* **7**: 2179.
- 607 Lun ATL, Chen Y, Smyth GK. (2016). It's DE-licious: A Recipe for Differential Expression
608 Analyses of RNA-seq Experiments Using Quasi-Likelihood Methods in edgeR. In: Vol.
609 1418. *Methods in Molecular Biology*. pp 391–416.
- 610 Makhalanyane TP, Valverde A, Gunnigle E, Frossard A, Ramond J-B, Cowan DA. (2015).
611 Microbial ecology of hot desert edaphic systems. *FEMS Microbiol Rev* **39**: 203–21.
- 612 Makhalanyane TP, Valverde A, Lacap DC, Pointing SB, Tuffin MI, Cowan DA. (2013).
613 Evidence of species recruitment and development of hot desert hypolithic
614 communities. *Environ Microbiol Rep* **5**: 219–24.
- 615 McCarthy DJ, Chen Y, Smyth GK. (2012). Differential expression analysis of multifactor
616 RNA-Seq experiments with respect to biological variation. *Nucleic Acids Res* **40**: 4288–
617 97.

- 618 McKinlay JB, Harwood CS. (2010). Carbon dioxide fixation as a central redox cofactor
619 recycling mechanism in bacteria. *Proc Natl Acad Sci U S A* **107**: 11669–75.
- 620 van der Meer MTJ, Schouten S, Bateson MM, Nübel U, Wieland A, Kühl M, *et al.* (2005).
621 Diel variations in carbon metabolism by green nonsulfur-like bacteria in alkaline
622 siliceous hot spring microbial mats from Yellowstone National Park. *Appl Environ*
623 *Microbiol* **71**: 3978–86.
- 624 Merrick MJ, Edwards RA. (1995). Nitrogen control in bacteria. *Microbiol Rev* **59**: 604–
625 22.
- 626 Meyer F, Paarmann D, D’Souza M, Olson R, Glass E, Kubal M, *et al.* (2008). The
627 metagenomics RAST server – a public resource for the automatic phylogenetic and
628 functional analysis of metagenomes. *BMC Bioinformatics* **9**: 386.
- 629 Nielsen KM, Calamai L, Pietramellara G. (2006). Stabilization of Extracellular DNA and
630 Proteins by Transient Binding to Various Soil Components. In: *Nucleic Acids and*
631 *Proteins in Soil*. Springer Berlin Heidelberg, pp 141–157.
- 632 Normand P, Benson DR, Normand P, Benson DR. (2015). *Geodermatophilus*. In:
633 *Bergey’s Manual of Systematics of Archaea and Bacteria*. John Wiley & Sons, Ltd:
634 Chichester, UK, pp 1–4.
- 635 Ottesen EA, Young CR, Eppley JM, Ryan JP, Chavez FP, Scholin CA, *et al.* (2013). Pattern
636 and synchrony of gene expression among sympatric marine microbial populations.
637 *Proc Natl Acad Sci U S A* **110**: E488-97.
- 638 Ottesen EA, Young CR, Gifford SM, Eppley JM, Marin R, Schuster SC, *et al.* (2014).
639 Multispecies diel transcriptional oscillations in open ocean heterotrophic bacterial

- 640 assemblages. *Science* (80-) **345**: 207–212.
- 641 Palmer FE, Emery DR, Stemmler J, Staley JT. (1987). Survival and growth of
642 microcolonial rock fungi as affected by temperature and humidity. *New Phytol* **107**:
643 155–162.
- 644 Palovaara J, Akram N, Baltar F, Bunse C, Forsberg J, Pedrós-Alió C, *et al.* (2014).
645 Stimulation of growth by proteorhodopsin phototrophy involves regulation of central
646 metabolic pathways in marine planktonic bacteria. *Proc Natl Acad Sci U S A* **111**:
647 E3650-8.
- 648 Pinto R, Tang QX, Britton WJ, Leyh TS, Triccas JA. (2004). The *Mycobacterium*
649 *tuberculosis* *cysD* and *cysNC* genes form a stress-induced operon that encodes a tri-
650 functional sulfate-activating complex. *Microbiology* **150**: 1681–1686.
- 651 Pointing SB, Belnap J. (2012). Microbial colonization and controls in dryland systems.
652 *Nat Rev Microbiol* **10**: 551–562.
- 653 Pratscher J, Dumont MG, Conrad R. (2011). Ammonia oxidation coupled to CO₂ fixation
654 by archaea and bacteria in an agricultural soil. *Proc Natl Acad Sci U S A* **108**: 4170–5.
- 655 R Core Team. (2017). R: A language and environment for statistical computing.
- 656 Rainey FA, Ray K, Ferreira M, Gatz BZ, Nobre MF, Bagaley D, *et al.* (2005). Extensive
657 diversity of ionizing-radiation-resistant bacteria recovered from Sonoran Desert soil
658 and description of nine new species of the genus *Deinococcus* obtained from a single
659 soil sample. *Appl Environ Microbiol* **71**: 5225–35.
- 660 Ramond J-B, Woodborne S, Hall G, Seely M, Cowan DA. (2018). Namib Desert primary
661 productivity is driven by cryptic microbial community N-fixation. *Sci Rep* **8**: 6921.

- 662 Rashid AM, Batey SFD, Syson K, Koliwer-Brandl H, Miah F, Barclay JE, *et al.* (2016).
663 Assembly of α -Glucan by GlgE and GlgB in Mycobacteria and Streptomyces.
664 *Biochemistry* **55**: 3270–3284.
- 665 Reich P, Numbem S, Almaraz R, Eswaran H. (2001). Land resource stresses and
666 desertification in Africa. In: Bridges EM, Hannam ID, Oldeman LR, Pening de Vries FWT,
667 Scherr SJ, S. S (eds). *Responses to Land Degradation. Proc. 2nd. International*
668 *Conference on Land Degradation and Desertification, Khon Kaen, Thailand*. Oxford
669 Press: New Delhi, India.
- 670 Reysenbach A, Pace NR. (1995). Archaea: a laboratory manual. In: Robb F, Place A (eds).
671 *Archaea: a laboratory manual*. Cold Spring Harbor press: New York, NY, pp 101–107.
- 672 Robinson MD, McCarthy DJ, Smyth GK. (2010). edgeR: a Bioconductor package for
673 differential expression analysis of digital gene expression data. *Bioinformatics* **26**: 139–
674 140.
- 675 Robinson MD, Oshlack A. (2010). A scaling normalization method for differential
676 expression analysis of RNA-seq data. *Genome Biol* **11**: R25.
- 677 Ronca S, Ramond J-B, Jones BE, Seely M, Cowan DA. (2015). Namib Desert
678 dune/interdune transects exhibit habitat-specific edaphic bacterial communities. *Front*
679 *Microbiol* **6**: 845.
- 680 Scherer S, Ernst A, Chen T-W, Böger P. (1984). Rewetting of drought-resistant blue-
681 green algae: Time course of water uptake and reappearance of respiration,
682 photosynthesis, and nitrogen fixation. *Oecologia* **62**: 418–423.
- 683 Schmieder R, Edwards R. (2011). Quality control and preprocessing of metagenomic

- 684 datasets. *Bioinformatics* **27**: 863–864.
- 685 Scholz H. (1972). The soils of the central Namib desert with special consideration of the
686 soils in the vicinity of Gobabeb. *Madoqua* **1972**: 33–51.
- 687 Schowanek D, Verstraete W. (1990). Phosphonate utilization by bacteria in the
688 presence of alternative phosphorus sources. *Biodegradation* **1**: 43–53.
- 689 Schulze-Makuch D, Wagner D, Kounaves SP, Mangelsdorf K, Devine KG, de Vera J-P, *et*
690 *al.* (2018). Transitory microbial habitat in the hyperarid Atacama Desert. *Proc Natl*
691 *Acad Sci U S A* **115**: 2670–2675.
- 692 Scola V, Ramond J-B, Frossard A, Zablocki O, Adriaenssens EM, Johnson RM, *et al.*
693 (2017). Namib Desert Soil Microbial Community Diversity, Assembly, and Function
694 Along a Natural Xeric Gradient. *Microb Ecol* **1**–11.
- 695 Seely M, Pallet J. (2008). Namib: Secrets of a desert uncovered. Venture Publications:
696 Windhoek, Namibia.
- 697 Sellstedt A, Richau KH. (2013). Aspects of nitrogen-fixing Actinobacteria, in particular
698 free-living and symbiotic *Frankia*. *FEMS Microbiol Lett* **342**: 179–86.
- 699 Sghaier H, Hezbri K, Ghodhbane-Gtari F, Pujic P, Sen A, Daffonchio D, *et al.* (2016).
700 Stone-dwelling actinobacteria *Blastococcus saxosidens*, *Modestobacter marinus* and
701 *Geodermatophilus obscurus* proteogenomes. *ISME J* **10**: 21–29.
- 702 Shannon P, Markiel A, Ozier O, Baliga NS, Wang JT, Ramage D, *et al.* (2003). Cytoscape:
703 A Software Environment for Integrated Models of Biomolecular Interaction Networks.
704 *Genome Res* **13**: 2498–2504.
- 705 Stomeo F, Valverde A, Pointing SB, McKay CP, Warren-Rhodes KA, Tuffin MI, *et al.*

- 706 (2013). Hypolithic and soil microbial community assembly along an aridity gradient in
707 the Namib Desert. *Extremophiles* **17**: 329–37.
- 708 Štoviček A, Kim M, Or D, Gillor O. (2017). Microbial community response to hydration-
709 desiccation cycles in desert soil. *Sci Rep* **7**: 45735.
- 710 Szymanski M, Zielezinski A, Barciszewski J, Erdmann VA, Karlowski WM. (2016).
711 5SRNadb: an information resource for 5S ribosomal RNAs. *Nucleic Acids Res* **44**: D180–
712 D183.
- 713 Tyx RE, Roche-Hakansson H, Hakansson AP. (2011). Role of dihydrolipoamide
714 dehydrogenase in regulation of raffinose transport in *Streptococcus pneumoniae*. *J*
715 *Bacteriol* **193**: 3512–24.
- 716 Vikram S, Guerrero LD, Makhalanyane TP, Le PT, Seely M, Cowan DA. (2016).
717 Metagenomic analysis provides insights into functional capacity in a hyperarid desert
718 soil niche community. *Environ Microbiol* **18**: 1875–1888.
- 719 Warren-Rhodes KA, Rhodes KL, Pointing SB, Ewing SA, Lacap DC, Gómez-Silva B, *et al.*
720 (2006). Hypolithic Cyanobacteria, Dry Limit of Photosynthesis, and Microbial Ecology in
721 the Hyperarid Atacama Desert. *Microb Ecol* **52**: 389–398.
- 722 White AK, Metcalf WW. (2007). Microbial Metabolism of Reduced Phosphorus
723 Compounds. *Annu Rev Microbiol* **61**: 379–400.
- 724 Zablocki O, Adriaenssens EM, Cowan D. (2015). Diversity and Ecology of Viruses in
725 Hyperarid Desert Soils. *Appl Environ Microbiol* **82**: 770–7.

726 Zarzycki J, Fuchs G. (2011). Coassimilation of organic substrates via the autotrophic 3-
727 hydroxypropionate bi-cycle in *Chloroflexus aurantiacus*. *Appl Environ Microbiol* **77**:
728 6181–8.

Figure 1

bioRxiv preprint first posted online Oct. 3, 2018; doi: <http://dx.doi.org/10.1101/432427>. The copyright holder for this preprint (which was not peer-reviewed) is the author/funder, who has granted bioRxiv a license to display the preprint in perpetuity. It is made available under a [CC-BY-NC-ND 4.0 International license](https://creativecommons.org/licenses/by-nc-nd/4.0/).

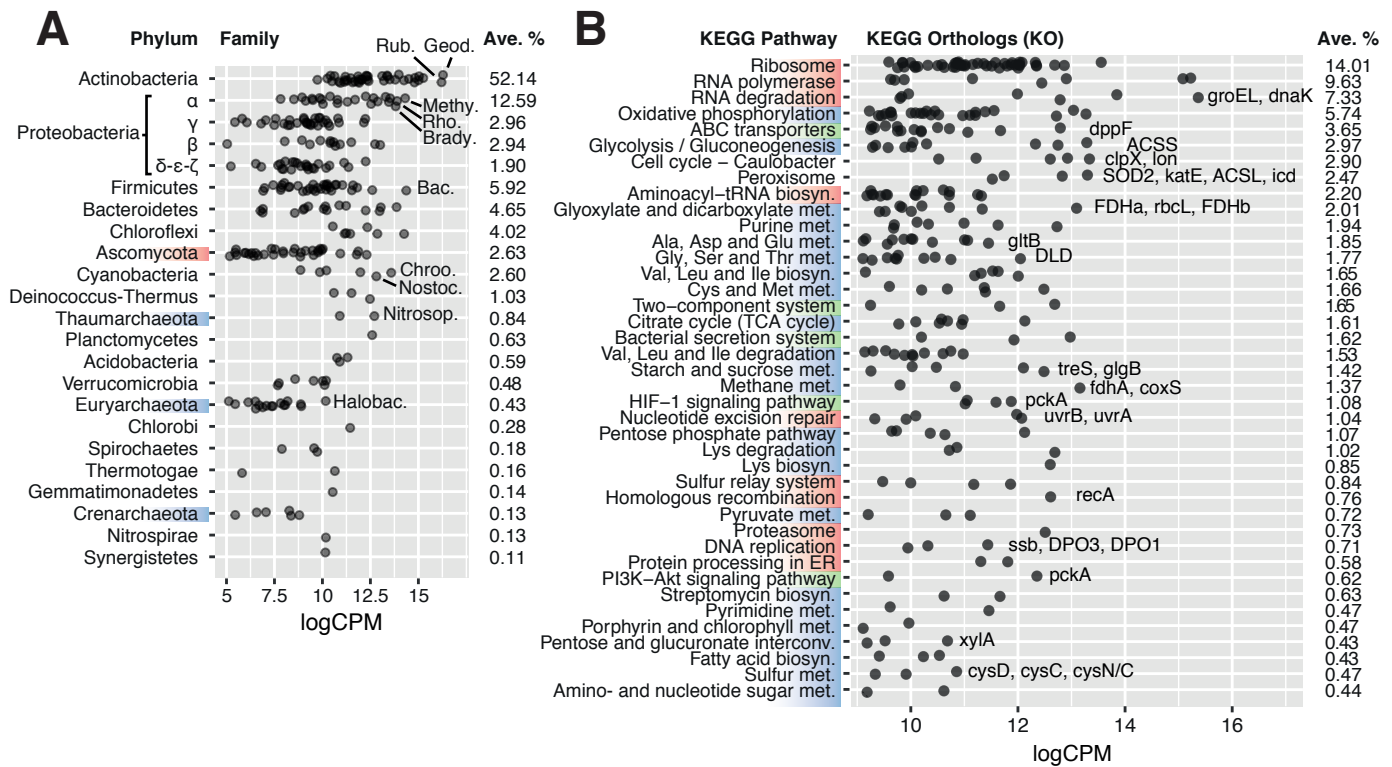


Figure 2

bioRxiv preprint first posted online Oct. 3, 2018; doi: <http://dx.doi.org/10.1101/432427>. The copyright holder for this preprint (which was not peer-reviewed) is the author/funder, who has granted bioRxiv a license to display the preprint in perpetuity. It is made available under a [CC-BY-NC-ND 4.0 International license](https://creativecommons.org/licenses/by-nc-nd/4.0/).

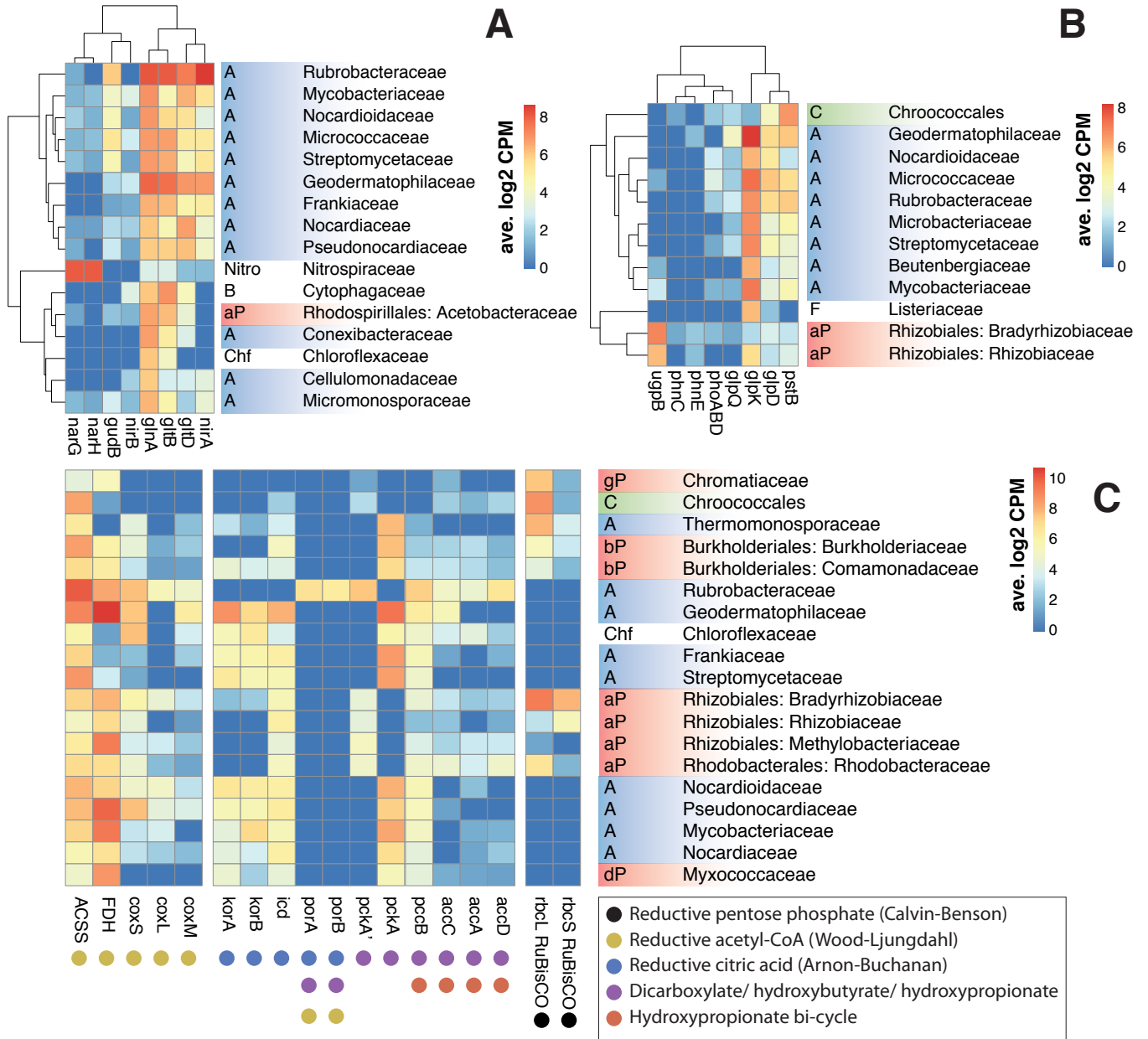


Figure 3

bioRxiv preprint first posted online Oct. 3, 2018; doi: <http://dx.doi.org/10.1101/432427>. The copyright holder for this preprint (which was not peer-reviewed) is the author/funder, who has granted bioRxiv a license to display the preprint in perpetuity. It is made available under a [CC-BY-NC-ND 4.0 International license](https://creativecommons.org/licenses/by-nc-nd/4.0/).

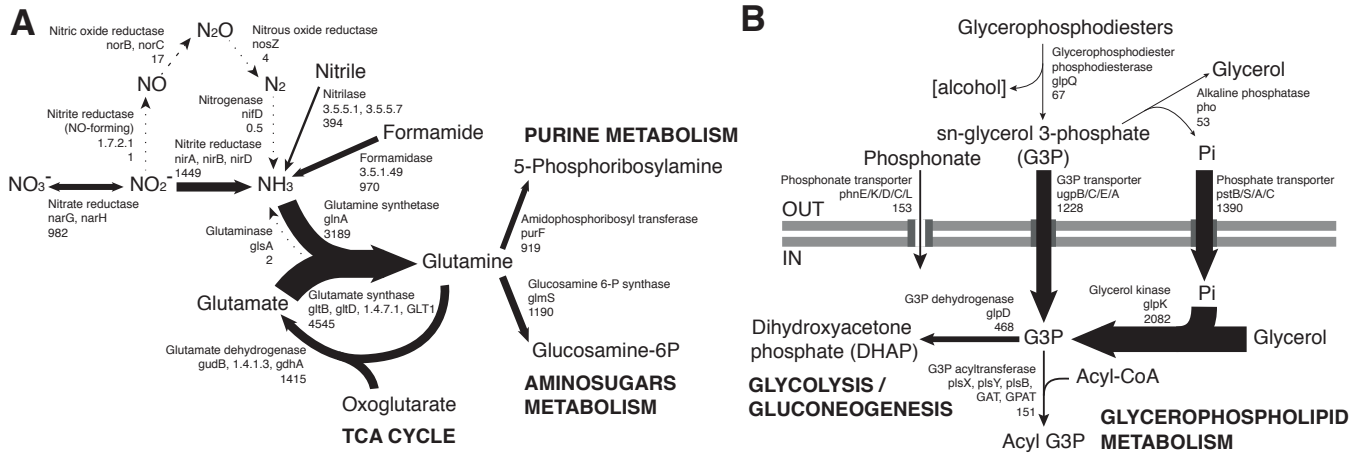


Figure 4

